Korean J. Chem. Eng., **29**(6), 750-755 (2012)
DOI: 10.1007/s11814-011-0264-5

Parameter estimation in multiple contact CO_2 miscibility simulation with uncertain experimental core flooding data

Sunil Kwon* and Wonsuk Lee,†**

*Department of Natural Resources and Environmental Eng., Dong-A University, Busan 133-791, Korea
**Korea Institute of Geoscience and Mineral Resources, Daejeon 305-350, Korea
(*Received 28 July 2011 • accepted 11 October 2011*)

Abstract−CO_2 flooding, which is an efficient method of enhanced oil recovery, is a very complicated process involving phase behavior. To understand the performance of CO_2 flooding and provide accurate data for designing reservoir development, a comprehensive investigation of the phase behavior of CO_2 miscible flooding and an accurate compositional reservoir simulation needs to be conducted. In PVT modeling, an effective and more physically reasonable equation of state model was achieved and the feasibility of CO_2 miscible flooding was determined by multiple contact minimum miscibility pressure (MCMMP) calculation. Furthermore, compositional reservoir simulation studies for predicting CO_2 miscible performance were designed and constructed with core flooding data. By matching with laboratory core flooding data, we can estimate parameters with uncertainty. The objective of this study was to find a work flow for parameter estimation in CO_2 miscible flooding process that can be used to design and optimize field CO_2 miscible floods.

Key words: CO_2 Injection, Miscible Flooding, Simulation, History Mmatching

INTRODUCTION

Enhanced oil recovery is a term applied to methods used for recovering oil from a petroleum reservoir beyond that recoverable by primary and secondary methods. The main objective of all methods of EOR is to increase the volumetric sweep efficiency and to enhance the displacement efficiency as compared to an ordinary water flooding. CO_2 miscible flooding as a tertiary recovery process is a mechanism with which to recover more oil, extend the field life and increase the profitability of the fields.

CO_2 injection is receiving increasing consideration for application to enhanced oil recovery (EOR) in both new reservoirs, and reservoirs that have been previously depleted and/or water flooded [1]. There is great potential for CO_2 injection for improved oil recovery; additionally, there is environmental and economic interest from a number of industrial sources in using CO_2 injection in depleted reservoirs to store CO_2 in order to alleviate the effects of CO_2 on global warming caused by CO_2 emissions. In over 30 years' production practice, CO_2 flooding has become the leading enhanced oil recovery technique for light and medium oils [2,3].

Depending on the properties of the reservoir fluids at reservoir conditions, the displacement of oil by CO_2 gas injection can be classified as both a miscible and immiscible process. A miscible or multiple contact miscible process occurs at pressures above the minimum miscibility pressure (MMP), in which there is more interchange of components. Immiscible displacement occurs at pressures below the MMP, in which there is less interchange of components or mixing zones between the injected gas and the reservoir fluid. CO_2 miscible flooding improves oil recovery through gas drive, swelling of the oil, and decreasing its viscosity [4]. Miscible injection is a proven, economically viable process that significantly increases oil recovery from many different types of reservoirs [5]. Theoretically, under CO_2 miscible flooding, CO_2 becomes completely miscible with the resident oil reducing the interfacial tension between them to zero, eliminating the capillary pressure and resulting in 0% residual oil saturation. Many of the current CO_2 EOR floods operate near the miscibility conditions to mobilize the maximum amount of incremental oil. In spite of all the advantages of the CO_2 process, however, it has the disadvantage of a high mobility ratio so that the CO_2 has a strong tendency to channel through the oil, bypassing much of the oil in the reservoir. To alleviate this difficulty, the injected CO_2 is often used in combination with water, in an alternating way (water alternating gas, WAG) in order to obtain the joint benefits of mobilizing oil with the miscible gas while using water to sweep mobilized oil to producing wells [6].

CO_2 flooding process involves very complicated phase behavior that depends on the PVT and fluids properties. To understand the performance of CO_2 flooding and provide accurate data for designing reservoir development, a comprehensive investigation of the phase behavior of CO_2 miscible flooding and accurate compositional reservoir simulation studies need to be conducted.

The objective of this study was to find a work flow for parameter estimation in CO_2 miscible flooding process that can be used to design and optimize field CO_2 miscible floods. To accomplish this, PVT experimental data were analyzed and reservoir simulation studies were conducted based on CO_2 flooding laboratory data. Through the history matching process, the assumed relative permeability curves with uncertainty were adjusted for model calibration.

CO_2 MISCIBLE FLOODING

The injection fluid (solvent) is normally natural gas, enriched natural gas, flue gas, nitrogen or CO_2 in miscible flooding. These

†To whom correspondence should be addressed.
E-mail: wslee@kigam.re.kr

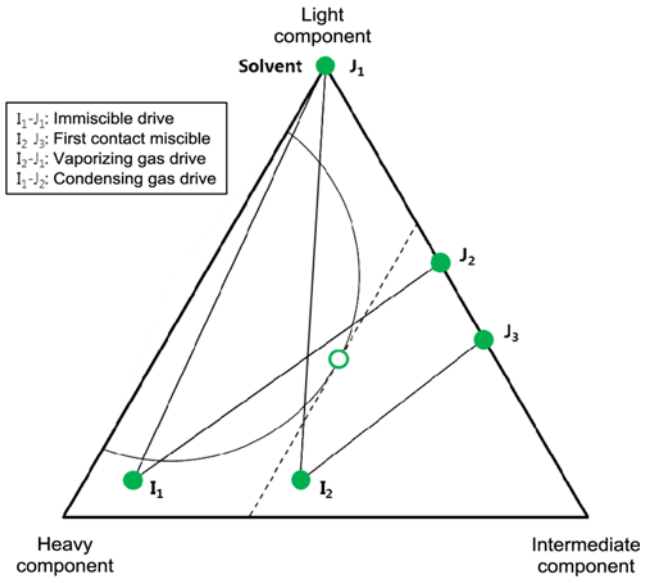

Fig. 1. Conditions for different types of oil displacement by solvents [7].

fluids are not the first contact with reservoir oils, but with a sufficiently high reservoir pressure, they achieve dynamic miscibility with many reservoir oils. To explain the different processes in miscible flooding, ternary diagrams are widely used as shown in Fig. 1. Since the dilution path (I_2-J_3) does not pass through the two-phase region or cross the critical tie line, it forms first contact miscible displacement. When the initial and injected compositions are on the opposite side of the critical tie line, the displacement is either a vaporizing gas drive (I_2-J_1) or a condensing gas drive (I_1-J_2). The degree of miscibility between a reservoir oil and injection gas is often expressed in terms of the minimum miscibility pressure (MMP). The multiple contact miscibility pressure is the lowest pressure at which the oil and gas phases resulting from a multiple contact process, vaporizing or condensing, between reservoir oil and an injection gas are miscible [7].

The pressure required for achieving dynamic miscibility with CO_2 is usually significantly lower than the pressure required for other gases such as natural gas, flue gas or nitrogen. The dynamic miscibility with CO_2 does not require the presence of intermediate molecular weight hydrocarbons in the reservoir fluid. The extraction of a broad range of hydrocarbons from the reservoir oil often causes dynamic miscibility to occur at attainable pressures, which are lower than the miscibility pressure for a dry hydrocarbon gas.

PVT MODELING OF CRUDE OIL-CO_2 SYSTEMS

The components of a fluid sample and experimental result data like DL (differential liberation), and a swelling test from CMG [8] are shown in Tables 1, 3, and 4, respectively. The results of the DL test provide a means of calculating the oil formation volume factors and gas solubility as a function of reservoir pressure. If a reservoir is to be depleted under gas injection or a dry gas cycling scheme, swelling tests should be performed. The purpose of this experiment was to determine the degree to which the proposed injection gas will dissolve in the hydrocarbon mixtures [9].

Table 1. Component of oil sample

Component	Mole fraction	Component	Mole fraction
H_2S	0.0027	FC16	0.0151
CO_2	0.0101	FC17	0.0134
N_2	0.0018	FC18	0.0129
C1	0.1257	FC19	0.0114
C2	0.0699	FC20	0.0089
C3	0.0664	FC21	0.0075
IC4	0.0235	FC22	0.0060
NC4	0.0471	FC23	0.0055
IC5	0.0282	FC24	0.0050
NC5	0.0514	FC25	0.0049
FC6	0.0472	FC26	0.0031
FC7	0.0444	FC27	0.0029
FC8	0.0493	FC28	0.0019
FC9	0.0299	FC29	0.0011
FC10	0.0404	NC7	0.0081
FC11	0.0316	NC8	0.0314
FC12	0.0254	NC9	0.0021
FC13	0.0255	C6H6	0.0019
FC14	0.0207	CC6	0.0278
FC15	0.0186	C30+	0.0693

*C30+: SG (0.97), MW (400)

Table 2. Seven pseudo-components of oil sample

Component	Components	Mole fraction
Pseudo 1	H_2S, CO_2	0.0128
Pseudo 2	N_2, C1	0.1275
Pseudo 3	C2, C3, IC4, NC4	0.2069
Pseudo 4	IC5, NC5, FC6, FC7	0.1712
Pseudo 5	FC8, FC9, FC10, FC11, FC12	0.1766
Pseudo 6	FC13, FC14, FC15, FC16, FC17, FC18, FC19, FC20	0.1265
Pseudo 7	FC21~FC29, NC7~NC9, C6H6, CC6, C30+	0.1785

In compositional simulation, the cost and computing time can increase significantly with the number of components in the system. Therefore, the original components in Table 1 were reduced to seven pseudo-components in Table 2 according to mole fraction. Phase behavior models may predict highly erroneous results, because the reduced pseudo-components are not fully defined. The current approach in the industry when encountering these erroneous results is to calibrate, or tune, an EOS model against experimental data generated at pertinent conditions for specific field studies. In the tuning process, the Peng Robinson (PR) equation of state (EOS) was used, and regression variables such as critical pressure, temperature, acentric factor, molecular weight, and volume shift parameters for the heaviest component were adjusted and tested using commercial phase behavior software, WinProp of CMG. The results of the tuned models for some properties are shown in Figs. 2, 3, 4, and 5, respectively. The results clearly demonstrate that effective and more physically reasonable tuning was achieved.

Table 3. Laboratory results of DL test at 186 °F

Pressure (psia)	Solution gas/oil ratio (ft^3/bbl)	Relative oil volume	Incremental gas specific gravity	Deviation factor	Gas formation volume factor (ft^3/ft^3)	Oil viscosity (cp)	Calculated gas viscosity (cp)	Oil density (gm/cc)
740	299.3	1.219				0.65		0.742
615	270.6	1.209	0.820	0.9199	0.0275	0.68	0.0132	0.743
465	236.4	1.186	0.803	0.9393	0.0371	0.72	0.013	0.752
315	188.1	1.175	0.883	0.9478	0.0554	0.83	0.0125	0.766
190	140.4	1.155	1.072	0.9524	0.0927		0.0116	0.795
130	106.7	1.098	1.227	0.9558	0.1366	0.89	0.0110	0.803
15	0.0	1.027	1.621	0.9916	1.2346	1.65	0.0102	0.813

Table 4. Laboratory results of swelling test at 186 °F

Solvent mole fraction	Saturation pressure (psia)	Oil formation volume factor (rm^3/m^3)	Swelling factor (ratio)	GOR (m^3/m^3)	Density (g/cc)	Viscosity (cp)
0	740	1.18	1.00	44	0.753	0.850
0.108	900	1.21	1.03	67	0.739	0.832
0.297	1488	1.43	1.21	123	0.707	0.556
0.54	1985	1.82	1.54	277	0.626	0.288
0.803	2355	3.68	3.12	675	0.48	0.171

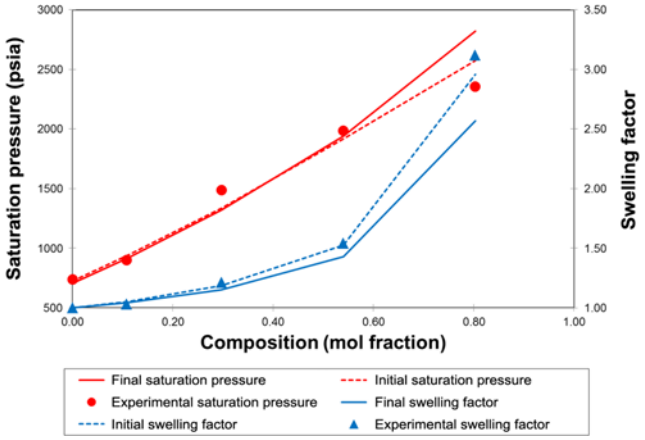

Fig. 2. Comparison of predicted saturation pressure and swelling factor in swelling test.

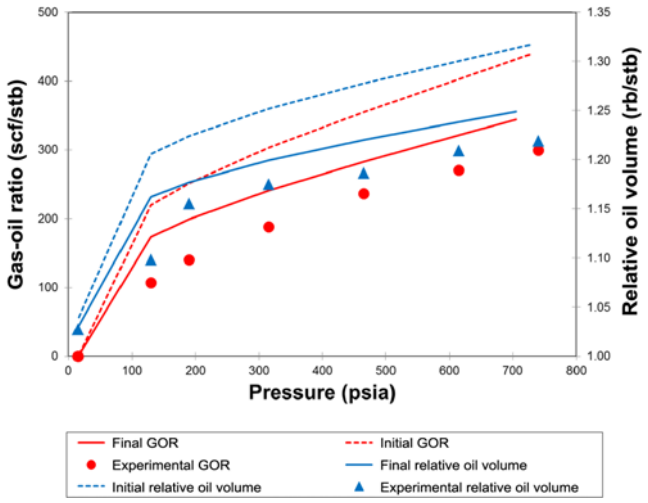

Fig. 3. Comparison of predicted GOR and relative oil volume in DL test.

Using the tuned pseudo-components, the multiple contact minimum miscibility pressure (MCMMP) was calculated in the case of 100% CO_2 injection. Input data such as reservoir temperature (186 °F), pressure (2,515 psia), and swelling test data (Table 4) were used in calculation. The MCMMP was achieved at 2,364.7 psia, which was lower than the reservoir pressure.

MATCHING WITH EXPERIMENTAL CORE FLOOD DATA

The reservoir simulation studies were conducted based on CO_2 flooding laboratory data [8] using CMG's GEM simulation software. Additionally, by matching with laboratory core flood data, we estimated parameters with uncertainty.

A CO_2 flooding experiment was performed using a length of 87.36 cm and a diameter of 3.745 cm. Table 5 gives the core properties and production conditions used for this study. An initial water saturation (connate water saturation) of 20% was established using formation water with a viscosity of 0.45 cp. In the core flooding test, the pressure and temperature were set as 2,500 psig and 186 °F, respectively, and the confining pressure was 5,650 psig. Water was injected before CO_2 injection at 10 cc/hr for 2.932 days, and then CO_2 was injected at 10 cc/hr for 3.030 days. Finally, chase water was injected at 10 cc/hr for 4.906 days.

To model the experiment with a 1D compositional model, we used 50×1×1 grid cells in each direction. At the production end, a production well is located where the minimum bottom hole pressure is set at 2,515 psi as an operating constraint. Because the rela-

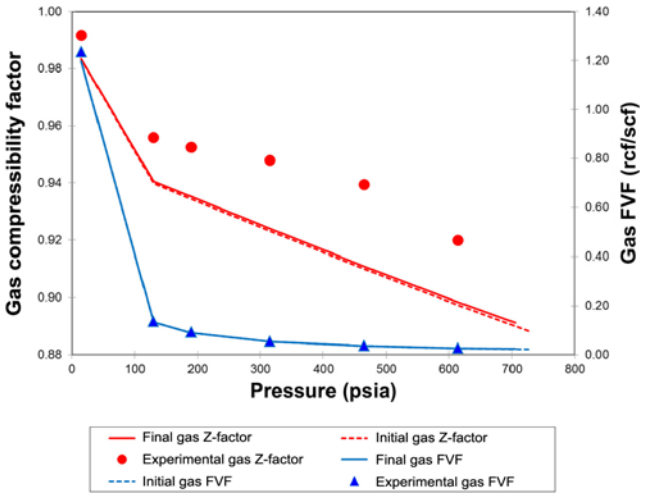

Fig. 4. Comparison of predicted gas compressibility and gas formation volume factor in DL test.

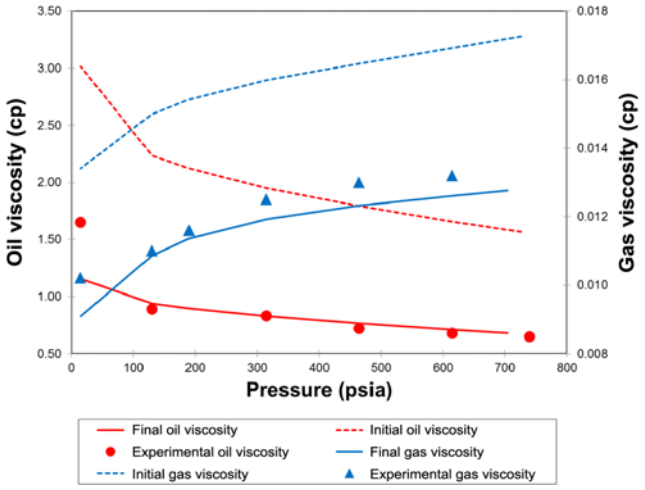

Fig. 5. Comparison of predicted oil and gas viscosity in DL test.

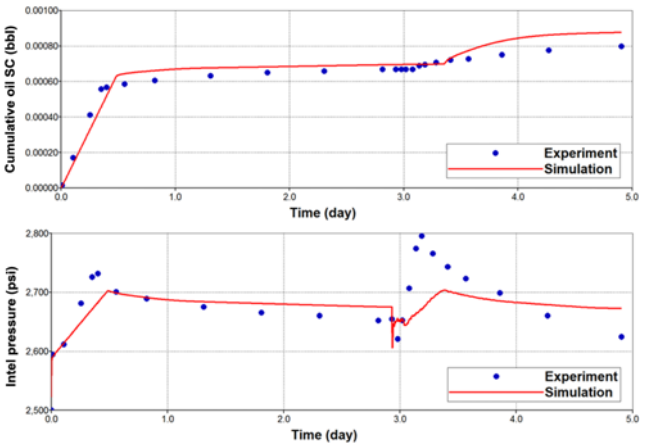

Fig. 6. Comparison of experimental and simulation results for cumulative oil production and inlet bottom hole pressure using assumed relative permeability parameters.

tive permeability curves were not experimentally measured, correlation equations by Stone's second model as normalized by Aziz and Settari [10] were used. In using correlation equations, end point parameters were initially assumed as in Table 6. Fig. 6 compares the experimental and simulation results for cumulative oil production and inlet bottom pressure. As shown in the figure, discrepancies between experimental and simulation results are observed. There are numerous possible causes for the differences between the experiment and simulation, some experimental and some related to our modeling process. However, the most subtle issue may be related to the relative permeability. Because we used correlation equations with assumed end point parameters, we tried to match the values measured in the laboratory by changing the curvature of the relative permeability curves, and by changing the end point saturation parameters.

To change the curvature of the relative permeability curves, the exponents (N_w, N_{ow}, N_{og}, and N_g) of k_{rw}, k_{row}, k_{rog}, and k_{rg} were se-

Table 5. Core properties and production conditions

Pore volume (cc)	234.55	Initial water saturation	0.2
Core depth (ft)	6200	Injection rate (cc/hr)	10.0
Porosity (fraction)	0.24	Production pressure (psig)	2500
Permeability (md)	11.43	Separator condition	14.7 psia at 60 °F
Rock compressibility (1/psi)	4.00E-6		
Core length (cm)	87.36		
Core diameter (cm)	3.75		

Table 6. Initial and optimum relative permeability parameters

Cases	N_w	N_{ow}	N_{og}	N_g	S_{gcrit}	S_{orw}	S_{org}	k_{rwiro}	k_{rgcl}
Initially assumed	2.0	2.0	2.0	2.0	0.00	0.25	0.00	0.080	0.02
1	4.0	2.0	3.0	3.0	0.03	0.27	0.05	0.085	0.015
2	4.0	2.0	3.0	3.0	0.02	0.27	0.03	0.085	0.015
3	4.0	2.0	3.0	3.0	0.05	0.27	0.03	0.085	0.020
4	4.0	2.0	3.0	3.0	0.05	0.28	0.03	0.085	0.020
5	4.0	2.0	3.0	3.0	0.05	0.28	0.05	0.085	0.015

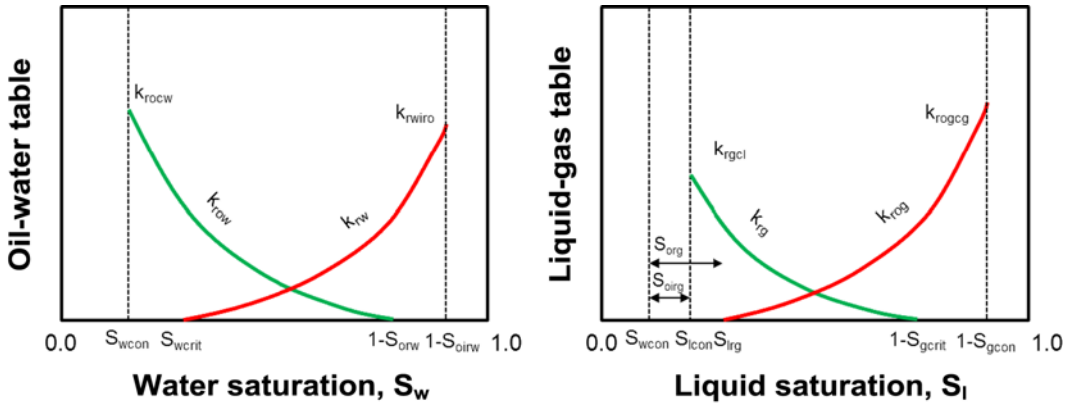

Fig. 7. Descriptions of relative permeability parameters used in Stone's second model.

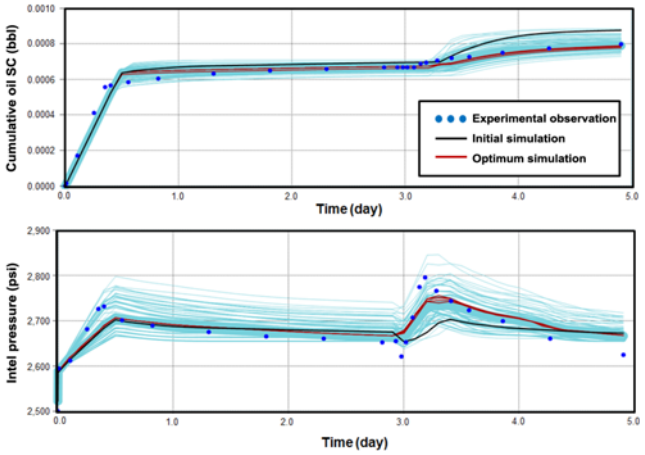

Fig. 8. Comparison of experimental and simulation results for cumulative oil production and inlet bottom hole pressure by changing relative permeability parameters.

lected as 1.5, 2.0, 3.0, 4.0, and 5.0 as presented in the following correlation equations. Also, the end point saturation parameters such as S_{orw}, S_{gcrit}, k_{rwiro}, and k_{rgcl}, which are described in Fig. 7, were changed.

$$k_{rw} = k_{wriro}\left[\frac{(S_w - S_{wcrit})}{(1.0 - S_{wcrit} - S_{oirw})}\right]^{N_w}, \quad (1)$$

$$k_{row} = k_{wocw}\left[\frac{(S_o - S_{orw})}{(1.0 - S_{wcon} - S_{orw})}\right]^{N_{ow}}, \quad (2)$$

$$k_{rog} = k_{rogcg}\left[\frac{(S_l - S_{org} - S_{wcon})}{(1.0 - S_{gcon} - S_{org} - S_{wcon})}\right]^{N_{og}}, \quad (3)$$

$$k_{rg} = k_{rgcl}\left[\frac{(S_g - S_{gcrit})}{(1.0 - S_{gcrit} - S_{oirg} - S_{wcon})}\right]^{N_g}, \quad (4)$$

After repeated simulation with various parameters, five optimum cases were found, as shown in Fig. 8, according to minimum square values between objective functions (cumulative oil production and pressure) and experimental data. The parameters of the five optimum cases are summarized in Table 6. Compared to the initial case, the five optimum cases subsequent to 3.0 days correlated very well with the experimental results. Fig. 9 shows the assumed and optimum (Case 5) relative permeability curves. In Fig. 9, the curvature of relative permeability curves has more influence on the parame-

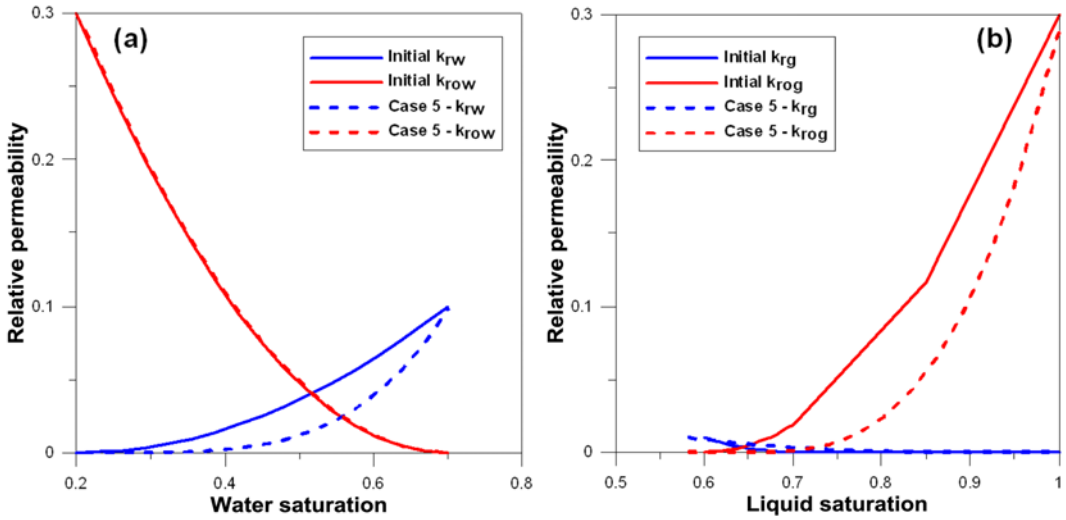

Fig. 9. Comparison of assumed and optimum relative permeability curves: (a) as a function of water saturation, (b) as a function of liquid saturation.

ters than on the end point saturations.

CONCLUSIONS

We developed a work flow for uncertain parameters in CO_2 miscible flooding by PVT modeling and reservoir simulation studies based on PVT and CO_2 core flooding experimental data. Finally, we estimated parameters with uncertainty by matching relative permeability curves. This could be used in the design and optimization of the CO_2 miscible flooding process. The following conclusions can be drawn from this study:

1. To decrease computing time in compositional simulation, the component numbers of fluid sample have to be reduced to pseudo-components. Because the reduced pseudo-components are not fully defined, the EOS model against experimental data needs to be calibrated. In the tuning process, by modifying the critical pressure, temperature, acentric factor, molecular weight, and volume shift parameters of the heaviest component as regression parameters, a more effective and physically reasonable EOS model was achieved.

2. For the feasibility of CO_2 miscible flooding in reservoir conditions, the multiple contact minimum miscibility pressure (MCMMP) was achieved at 2,364.7 psia. Because it is lower than reservoir pressure (2,515 psia), CO_2 miscible flooding could be a reasonable option for EOR of the reservoir.

Compositional reservoir simulation studies for predicting CO_2 miscible performance have been designed and conducted. By matching with laboratory core flooding data, we estimated parameters with uncertainty. We also found that the curvature of relative permeability curves has more influence on parameters than on end-point saturations.

ACKNOWLEDGEMENTS

This work was supported by the "Energy Efficiency & Resources" of the Korea Institute of Energy Technology Evaluation and Planning (KETEP) grant funded by the Korea government Ministry of Knowledge Economy.

NOMENCLATURE

k_{rw} : relative permeability to water in oil-water system
k_{row} : relative permeability to oil in oil-water system
k_{rg} : relative permeability to gas in liquid-gas system
k_{rog} : relative permeability to liquid in liquid-gas system
k_{rocw} : oil relative permeability at the connate water saturation
k_{rwiro} : water relative permeability at the residual oil saturation
k_{rgcl} : gas relative permeability at the connate liquid saturation
k_{rogcg} : liquid relative permeability at the residual liquid saturation
N_w, N_{ow}, N_{og}, N_g : exponents on relative permeability curves
S_{orw} : residual oil saturation in oil-water system
S_{oirw} : irreducible oil saturation in oil-water system
S_{org} : residual oil saturation in liquid-gas system
S_{oirg} : irreducible oil saturation in liquid-gas system
S_{gcrit} : critical gas saturation
S_{gcon} : connate gas saturation
S_{wcrit} : critical water saturation
S_{wcon} : connate water saturation

REFERENCES

1. DOE, *DOE's Oil Recovery R&D Program*, Fossil Energy (2006).
2. M. Dong, S. Huang and R. Srivastava, *JCPT*, November, 53 (2000).
3. R. B. Grigg and D. S. Schechter, SPE 38849 the SPE Annual Technical Conference and Exhibition, San Antonia, US (1997).
4. J. Bon, H. K. Kalfa and A. M. Theophilos, SPE 97536 the SPE International Improved Oil Recovery Conference in Asia Pacific, KL, Malaysia (2005).
5. E. D. Holstein and F. I. Stalkup, *SPE Petroleum engineering handbook Vol. 5*, Richardson Texas (2007).
6. S. Ghedan, SPE 125581 the SPE/EAGE Reservoir Characterization and Simulation Conference, Abu Dhabi, UAE (2009).
7. L. W. Lake, *Enhanced oil recovery*, University of Texas and Austin (1989).
8. CMG, *Enhanced oil recovery with miscible CO_2 injection in IMEX & GEM*, CMG Training Course (2010).
9. T. H. Ahmed, *Equations of state and PVT analysis*, Gulf Publishing Company, Houston Texas (2007).
10. K. Aziz and A. Settari, Petroleum Reservoir Simulation, Applied Science Publishers, London (1979).